

Mechanical Characterization of Seismic Base Isolation Elastomers

R. F. KULAK, T. H. HUGHES
Argonne National Laboratory, Argonne, IL USA

1 INTRODUCTION

From the various devices proposed for seismic isolators, the laminated elastomer bearing is emerging as the preferred device for large buildings/structures, such as nuclear reactor plants. The laminated bearing is constructed from alternating thin layers of elastomer and metallic plates (shims). The elastomer is usually a carbon filled natural rubber that exhibits damping when subjected to shear. Recently, some blends of natural and synthetic rubbers have appeared. Before candidate elastomers can be used in seismic isolation bearings, their response to design-basis loads and beyond-design-basis loads must be determined. This entails the development of constitutive models and then the determination of associated material parameters through specimen testing.

This paper describes the methods used to obtain data for characterizing the mechanical response of elastomers used for seismic isolation. The data provides a data base for use in determining material parameters associated with nonlinear constitutive models. In addition, the paper presents a definition for a damping ratio that does not exhibit the usual reduction at higher strain-level cycles.

2 CONSTITUTIVE MODEL

Several constitutive models have been proposed to simulate the behavior of elastomeric materials. Koh and Kelly (1985) use a fractional derivative representation, and Simo and Taylor (1985) use a viscoelastic model with damage effects. In the Simo-Taylor model, the stress tensor, σ_{ij} , is given by

$$\sigma_{ij} = K \ln J \delta_{ij} + \int_{-\infty}^{t_0} [G_\infty + (G_0 - G_\infty)e^{-(t-s)/\nu}] \dot{\pi}_{ij}(s) ds \quad (1)$$

where K is the bulk modulus, J the determinant of the deformation gradient, δ_{ij} the identity tensor, G_∞ and G_0 the long term and short term shear moduli, respectively, t is the time, and ν is the relaxation time constant. The strain history function is expressed by

$$\pi_{ij}(s) = \left[\beta - (1-\beta) \frac{1-e^{\psi_s/\alpha}}{\psi_s/\alpha} \right] \text{dev } \bar{C}_{ij}(s) \quad (2)$$

where α and β are material parameters, ψ is the damage parameter, and \bar{C}_{ij} is the volume preserving right Cauchy strain tensor. Equations 1 and 2 identify six material parameters that must be obtained from specimen tests, namely: K , G_o , G_∞ , α , ν , and β .

3 DAMPING RATIO

One of the quantities normally used to characterize elastomers is the damping ratio, ξ . However, there is not a unique method for determining its value from experimental data. For example, a popular formula for the damping ratio is

$$\xi = \frac{U_d}{4\pi G' \gamma_{\max}^2} ; \quad U_d = \int_0^{2\pi/\omega} \tau \dot{\gamma} dt ; \quad G' = \frac{\tau(\gamma_{\max})}{\gamma_{\max}} \quad (3)$$

where U_d is the energy dissipated per cycle (i.e., the area within the hysteresis loop), G' the storage modulus, γ the shear strain, and τ the shear stress. Note, the storage modulus is defined to be the stress at the maximum strain. The above definition is obtained from a linear viscoelastic model and works well for those materials. It also provides reasonable values for elastomers at strain levels below 100 percent, which is the range where the hysteresis loops are reasonably elliptical. However, at higher levels the loops are no longer elliptical and Eq. 3 gives misleading results. To obtain more reasonable values for the damping ratio, the following definition can be used

$$\bar{\xi} = \frac{U_d}{4\pi U_s} ; \quad U_s = \int_0^{\varepsilon_{\max}} \bar{\tau} d\gamma \quad (4)$$

Here $\bar{\tau}$ defines the average value of the hysteresis loop at a fixed strain level. Thus, the $\bar{\tau}$ curve bisects the hysteresis loop and represents a pseudo elastic response curve. It should be noted that for linear viscoelastic materials, the $\bar{\tau}$ curve approximates the storage modulus line.

4 TESTING ENVIRONMENT

Small samples of the elastomer were tested in shear to obtain the mechanical data required to characterize the elastomers and to validate the constitutive model. The tests were conducted using an Instron model 8502 digital servohydraulic testing machine. A 386 PC computer is used for test supervision, data acquisition and analysis. The Instron machine uses full digital control of feedback, wave generation and all other functions using multiple

microprocessors. The PC computer program used to interface with the operator and analyze the data was written specifically for this type of elastomer testing by one of the authors. The test specimens consist of two elastomer pads 5 mm thick by 25 mm square mounted in the three bar lap configuration. The specimens are fabricated in a mold by bonding the elastomer to the steel bars during vulcanization. The elastomer tested for this paper is a high damping natural rubber compound provided by Oil States Industries of Arlington, Texas. It is identified as their proprietary compound #259-62.

Each test was performed at room temperature at a selected strain and frequency using a sine wave loading for six consecutive cycles. The values of shear modulus, damping, etc. reported here were calculated using the 100 data points from the hysteresis loop of the sixth cycle. Since the three-bar specimens contain two pads, the results represent an average for the two pads. As in most elastomer testing, the amount the specimen has been worked prior to the test can have a marked effect on the results. This will be noted in the discussion of the results since we had some difficulty in obtaining consistent values. Reference to a scragged state usually refers to a prior loading of approximately ten cycles at 0.5 Hz and the desired strain level or extensive testing within the past hour. Reference to an unscragged state usually indicates a 24 hour rest period.

5 RESULTS

For the purpose of characterizing the elastomer under a variety of conditions, the test specimens were subjected to several types of tests. The test results provide a data base for benchmarking constitutive models and comparing various elastomers.

The first test performed was a prescribed strain test in which the specimen was subjected to six cycles at each strain level. The following strain sequence was prescribed ± 5 , ± 10 , ± 20 , ± 50 , ± 100 , ± 150 , ± 200 , ± 250 , and ± 300 percent shear strain. Figure 1 shows the variation in stiffness with shear strain at 0.5 Hz. The stiffness reduces in value in the range of 0 to 100 percent and begins to increase in value at about 150 percent. The first cycle values were always greater than the sixth cycle. The variation in damping with strain is shown in Fig. 2. The difference in damping ratio as calculated by Eqs. 3 and 4 is also shown. The rubber specimen tests indicate that the energy dissipation varied with the square of the strain. Figure 3 shows the hysteresis loop for the 300 percent test. The pseudo elastic response curve is shown by the dashed curve and the linear elastic response curve by the dotted line.

The second test performed was an up-down strain sequence test. This test was conducted by subjecting the specimen to a series of increasing strain levels followed by a series of decreasing strain levels. The specimen was subjected to six cycles of an increasing strain sequence (± 5 , ± 10 , ± 20 , ± 50 , ± 100 , ± 150 percent) immediately followed by six cycles of a decreasing strain sequence (± 100 , ± 50 , ± 20 , ± 10 , ± 5 percent). Table 1 gives the values for stiffness during the increasing strain sequence, decreasing strain sequence,

and the average of the two. It was noticed that the stiffness at a specific strain level is always less during the down sequence than during the up sequence. Also, the percent difference is greater at the lower strain levels.

The next test was performed to determine the variation in stiffness and damping with frequency. The specimens were tested at the following frequencies: 0.01, 0.1, 0.5, 0.8, 1, 5, and 10 Hz. The maximum strain at each frequency was limited by the performance envelope of the testing machine. For example, the 5 percent strain tests were performed at all frequencies, and the 150 percent strain tests were performed only up to 1.0 Hz. Figures 4 and 5 show the frequency dependence of the stiffness and damping. It is noted that for the seismic isolation system design frequency range (0.4 to 1.0 Hz), the variations in stiffness and damping are small. Also, these variations indicate that the material damping is close to being hysteretic.

A relaxation test was performed to determine the elastomer's behavior under constant strain. A shear strain of 100 percent was applied to the specimen and held for 165 minutes. The resulting stress relaxation is shown in Fig. 6. It is seen that the stress drops rapidly from its initial value of 105 psi to 84 psi at 165 minutes.

ACKNOWLEDGMENTS

The support of Mr. R. Seidensticker and Dr. Y. Chang is greatly appreciated. The assistance of Mr. Fiala is also acknowledged. This work was performed under the auspices of the U.S. Department of Energy, Office of Technology Support Programs, under contract W-31-109-Eng-38.

REFERENCES

- Koh, C. G. and Kelly, J. M. (1985). Fractional Derivative Representation of Seismic Response of Base-Isolated Models: Theory and Experiments, UCB/SESM 85/07, University of California at Berkeley.
- Simo, J. C. and Taylor, R. L. (1985). A Three-Dimensional Finite Deformation Viscoelastic Model Accounting for Damage Effects, UCB/SESM/85-02, University of California at Berkeley.

Table 1. Difference in secant modulus between the up sequence and down sequence

Strain (%)	Up	Down	Average
5	343	312	327
10	266	248	257
20	207	196	201
50	146	140	143
100	116	112	114
150	121	121	121

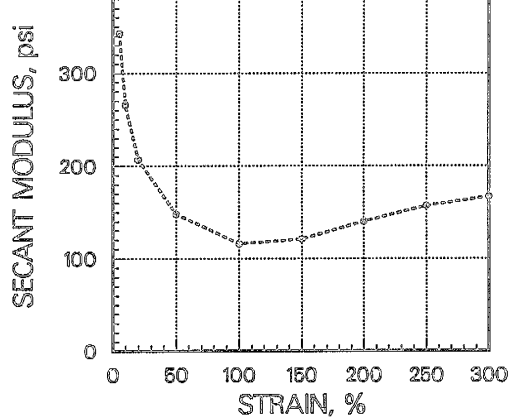


Fig. 1. Variation in stiffness with shear strain

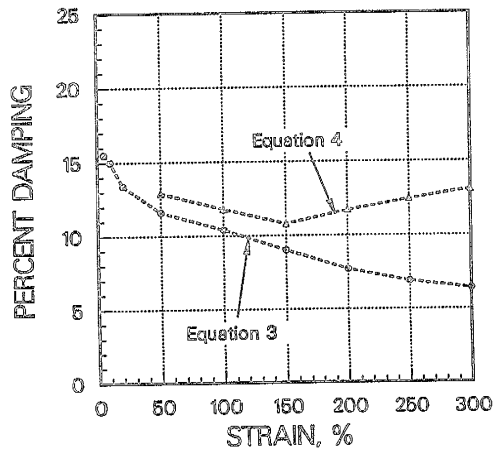


Fig. 2. Variation in damping with shear strain

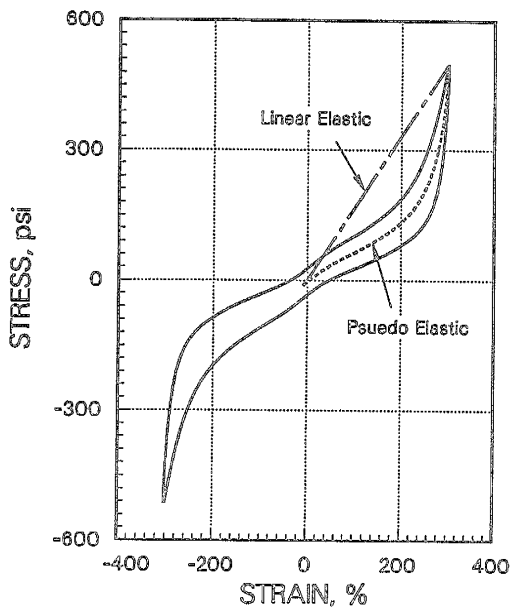


Fig. 3. Hysteresis loop for 300 percent shear strain

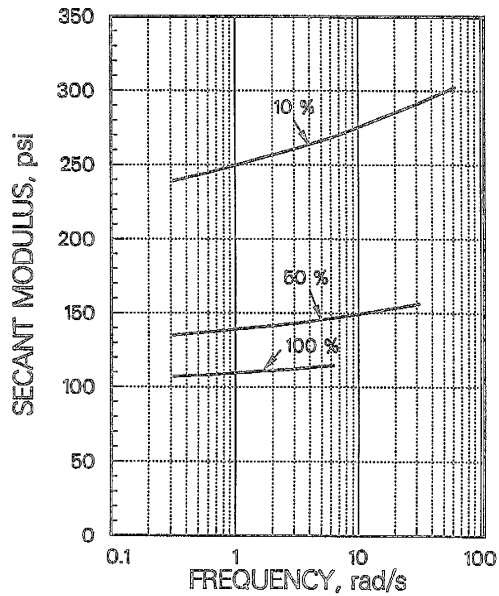


Fig. 4. Variation in stiffness with frequency and strain level

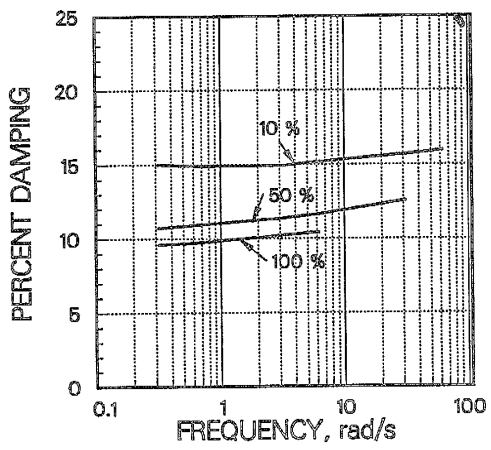


Fig. 5. Variation in damping with frequency and strain level

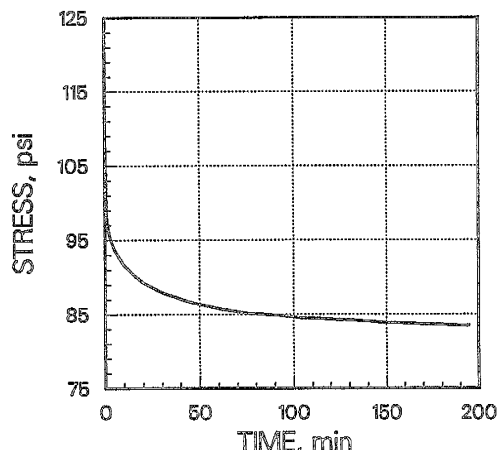


Fig. 6. Stress relaxation